Analytic study on a singularity interacting with a semi-infinite interfacial crack in a piezoelectric bimaterial

Ming-Ho Shen[1], Shih-Yu Hung[1], and Shih-Nung Chen[1]

[1] Department of Automation Engineering, Nan Kai University of Technology

Abstract

The interaction between a singularity and a semi-infinite interfacial crack in a piezoelectric bimaterial is studied using the extended Stroh formalism. The singularity considered here involves a line dislocation, a line force and a line charge. The crack surface is assumed to be mechanically free and electrically open. Based on the methods of mapping function, analytical continuation in conjunction with alternating technique, the complex potentials are derived in each medium of the anisotropic piezoelectric bimaterial. The generalized stress fields, generalized stress intensity factors and the image forces exerted on the dislocation are given explicitly. Numerical results demonstrate that the boundary conditions at the interface and the crack surface are satisfied. They also show the effects of the singularity and material combination on the generalized stress fields, generalized stress intensity factors and the image forces.

Keywords: Dislocation, Image forces, Stroh formalism, Alternating technique

1. Introduction

Due to the intrinsic electro-mechanical coupling behavior, piezoelectric materials such as ferroelectric ceramics can be widely used in modern device. These piezoelectric ceramics are brittle and in the manufacturing process easily produce micro-defects, such as dislocations, cracks, voids, etc. The existences defects induce high stress concentrations, which may greatly influence the performance of piezoelectric devices. The fundamental solutions for a dislocation and a concentrated force are significant since the dislocation solutions can be served as kernel functions for general crack and void problems. Barnett and Lothe (1975) extended the six-dimensional Stroh formalism to eight-dimensional formalism for solving the problem of a line dislocation and a line charge in anisotropic piezoelectric materials. Pak (1992) analyzed the piezoelectric cracks by a

distributed dislocation method. Meguid and Deng (1998) analyzed the problem of a screw dislocation interacting with an inhomogeneity in piezoelectric materials. Chung and Ting (1996), Liu et al. (1997) Hung and Kuang (2001) and Zhou et al. (2005) conducted an analysis on a line force and a line dislocation in anisotropic piezoelectric materials with an elliptic hole, crack or elliptic inhomogeneity etc. Lee et al. (2000) discussed the interaction between a semi-infinite crack and a screw dislocation under anti-plane mechanical and in-plane electrical loadings. Chen et al. (2002) studied a piezoelectric screw dislocation near a semi-infinite wedge crack. Chen et al. (2004) solved the problem of a line dislocation interacting with a semi-infinite crack in a piezoelectric solid. Yang et al (2007, 2008) used the dislocation solution to formulate the singular integral equations for solving the problem of a crack in a half-plane piezoelectric solid and the problem of an infinite sequence of parallel cracks in an infinite piezoelectric solid.

In piezoelectric composites, cracks usually propagate along the interface. The investigation of the problem involving interface cracks between two bonded dissimilar piezoelectric materials has attracted increasing attention. Suo et al. (1992) examined the problem of an interface crack between dissimilar anisotropic piezoelectric media and the dependence of singularities at the tips of an interface crack with respect to different electrical conditions. A circular-arc crack at the interface of a circular piezoelectric inclusion and a piezoelectric matrix under anti-plane shear and in-plane electric loading was considered by Zhong and Meguid (1997) and Deng and Meguid (1999), who derived complex series solution and closed-form solution, respectively. Wang and Shen (2002) give a general treatment on various interface defects at anisotropic piezoelectric bi-material interface. Gao et. al. (2004) presented the solutions for the problem of periodic interfacial cracks in two dissimilar piezoelectric materials. Hao and Liu (2006) investigated the interaction between a screw dislocation and a semi-infinite interfacial crack in a transversely isotropic magnetoelectro-elastic bi-material. The dislocation line is perpendicular to the isotropic basal plane of the bi-material. In the present paper, we investigate the plane problems for a line force, charge and dislocation interacting with a semi-infinite interfacial crack in anisotropic bi-materials. The analytical derivation is based on the extended Stroh formalism, conformal mapping and the analytical continuation technique which is alternatively applied across the bounded interface and crack surface.

2. Basic equations for two-dimensional piezoelectric problem

In a fixed rectangular coordinates system (x_1, x_2, x_3), the basic equations for linear piezoelectric materials can be written as

$$\sigma_{ij,j} = 0 \tag{1}$$

$$D_{i,i} = 0 \tag{2}$$

$$\gamma_{ij} = \frac{1}{2}(u_{i,j} + u_{j,i}) \tag{3}$$

$$E_i = -\varphi_{,i} \tag{4}$$

$$\sigma_{ij} = c_{ijkl}\gamma_{kl} - e_{kij}E_j \tag{5}$$

$$D_i = e_{ikl}\gamma_{kl} + \varepsilon_{ik}E_k \tag{6}$$

where repeated Latin indices mean summation and a comma stands for partial differentiation. c_{ijkl}, e_{kij} and ε_{ik} are the corresponding elastic, piezoelectric and dielectric constants. σ_{ij}, u_i, D_i, φ, γ_{ij} and E_i are stress, displacement, electric displacement, electric potential, strain and electric field, respectively. For two-dimensional problems in which all the variables depend on x_1 and x_2 only, following Suo et al. (1992), Chung and Ting (1996) and Zhou et al. (2005), the general solution is obtained by the linear combination of four complex analytical functions

$$\mathbf{u} = \mathbf{A}\mathbf{f}(z_k) + \overline{\mathbf{A}\mathbf{f}(z_k)} \tag{7}$$

$$\boldsymbol{\phi} = \mathbf{B}\mathbf{f}(z_k) + \overline{\mathbf{B}\mathbf{f}(z_k)} \tag{8}$$

where

$$\mathbf{u} = [u_1, u_2, u_3, \varphi]^t$$

$$\boldsymbol{\phi} = [\phi_1, \phi_2, \phi_3, \phi_4]^t$$

$$\mathbf{f}(z_k) = [f_1(z_1), f_2(z_2), f_3(z_3), f_4(z_4)]^t, \quad z_k = x_1 + p_k x_2, \quad k = 1, 2, 3, 4$$

In which ϕ_i are the generalized stress functions, $\mathbf{A}$ and $\mathbf{B}$ are 4×4 complex matrices related to the material constants, expressed as

$$\mathbf{A} = [\mathbf{a}_1, \mathbf{a}_2, \mathbf{a}_3, \mathbf{a}_4] \tag{9}$$

$$\mathbf{B} = [\mathbf{b}_1, \mathbf{b}_2, \mathbf{b}_3, \mathbf{b}_4] \tag{10}$$

The eigenvalues p_k and eigenvectors $\mathbf{a}_k$ are determined by the following equations

$$[\mathbf{Q} + (\mathbf{R} + \mathbf{R}^t)p + \mathbf{T}p^2]\mathbf{a} = 0 \tag{11}$$

where

$$\mathbf{Q} = \begin{bmatrix} c_{1111} & c_{1121} & c_{1131} & e_{121} \\ c_{1211} & c_{1221} & c_{1231} & e_{121} \\ c_{1311} & c_{1321} & c_{1331} & e_{131} \\ e_{111} & e_{121} & e_{131} & -\varepsilon_{11} \end{bmatrix} = \begin{bmatrix} c_{11} & c_{16} & c_{15} & e_{11} \\ c_{16} & c_{66} & c_{56} & e_{16} \\ c_{15} & c_{56} & c_{55} & e_{15} \\ e_{11} & e_{16} & e_{15} & -\varepsilon_{11} \end{bmatrix}$$

$$\mathbf{R} = \begin{bmatrix} c_{1112} & c_{1122} & c_{1132} & e_{211} \\ c_{1212} & c_{1222} & c_{1232} & e_{221} \\ c_{1312} & c_{1322} & c_{1332} & e_{231} \\ e_{112} & e_{122} & e_{132} & -\varepsilon_{12} \end{bmatrix} = \begin{bmatrix} c_{16} & c_{12} & c_{14} & e_{21} \\ c_{66} & c_{26} & c_{46} & e_{26} \\ c_{56} & c_{25} & c_{45} & e_{25} \\ e_{16} & e_{12} & e_{14} & -\varepsilon_{12} \end{bmatrix}$$

$$\mathbf{T} = \begin{bmatrix} c_{2112} & c_{2122} & c_{2132} & e_{212} \\ c_{2212} & c_{2222} & c_{2232} & e_{222} \\ c_{2312} & c_{2322} & c_{2332} & e_{232} \\ e_{212} & e_{222} & e_{232} & -\varepsilon_{22} \end{bmatrix} = \begin{bmatrix} c_{66} & c_{26} & c_{46} & e_{26} \\ c_{26} & c_{22} & c_{24} & e_{22} \\ c_{46} & c_{24} & c_{44} & e_{24} \\ e_{26} & e_{22} & e_{24} & -\varepsilon_{22} \end{bmatrix}$$

and the eigenvectors $\mathbf{b}_k$ can be obtained as

$$\mathbf{b}_k = (\mathbf{R}^t + p_k\mathbf{T})\mathbf{a}_k = -\frac{1}{p_k}(\mathbf{Q} + p_k\mathbf{R})\mathbf{a}_k \tag{12}$$

After the normalization for eigenvectors $\mathbf{A}$ and $\mathbf{B}$, the following relation can be obtained

$$\begin{bmatrix} \mathbf{B}^t & \mathbf{A}^t \\ \overline{\mathbf{B}}^t & \overline{\mathbf{A}}^t \end{bmatrix}\begin{bmatrix} \mathbf{A} & \overline{\mathbf{A}} \\ \mathbf{B} & \overline{\mathbf{B}} \end{bmatrix} = \begin{bmatrix} \mathbf{I} & 0 \\ 0 & \mathbf{I} \end{bmatrix} \tag{13}$$

The generalized stresses can be represented as

$$\boldsymbol{\sigma}_1 = [\sigma_{11}, \sigma_{12}, \sigma_{13}, D_1]^t = -[\phi_{1,2}, \phi_{2,2}, \phi_{3,2}, \phi_{4,2}]^t \tag{14}$$

$$\boldsymbol{\sigma}_2 = [\sigma_{21}, \sigma_{22}, \sigma_{23}, D_2]^t = [\phi_{1,1}, \phi_{2,1}, \phi_{3,1}, \phi_{4,1}]^t \tag{15}$$

If the traction and the normal component of electric displacement D_n are given on the boundary, the corresponding boundary condition can be expressed as

$$\boldsymbol{\phi}(z_k) = \mathbf{B}\mathbf{f}(z_k) + \overline{\mathbf{B}\mathbf{f}(z_k)} = \int_s \mathbf{t}\,ds, \quad \mathbf{t} = [t_1, t_2, t_3, D_n]^t \tag{16}$$

where t_k (k=1,2,3) are the components of surface traction.

3. A singularity in a homogeneous medium

In the previous section, it was shown that a general solution for a generalized two-dimensional piezoelectric problem can be expressed by four complex analytical functions $\mathbf{f}(z_k)$. Now we examine the solution $\mathbf{f}_0(z_k)$ of a singularity in a homogeneous medium. Let the generalized line dislocation $\mathbf{b}^p$ and the generalized line force $\mathbf{f}^p$ be applied at a point z_0, where $\mathbf{b}^p = [\mathbf{b}^t, b_\varphi]^t = [b_{x1}, b_{x2}, b_{x3}, b_\varphi]^t$, $\mathbf{b}$ represents Burgers vector and b_φ represents an electric potential jump across the slip plane, and $\mathbf{f}^p = [\mathbf{f}^t, q]^t = [f_{x1}, f_{x2}, f_{x3}, q]^t$, $\mathbf{f}$ represents a line force and q represents a line charge. The equilibrium conditions of the force and the single-valued conditions of the generalized displacement are

$$\oiint_c d\boldsymbol{\phi} = \mathbf{f}^p, \qquad \oiint_c d\mathbf{u} = \mathbf{b}^p \tag{17}$$

where c represents an arbitrary closed curve around the point z_0. We take the solution form for generalized line dislocation $\mathbf{b}^p$ and generalized line force $\mathbf{f}^p$ be applied at a point z_0 in an infinite homogeneous medium as

$$\mathbf{f}_0(z_k) = < \log(z_k - z_{k0}) > \mathbf{p} \tag{18}$$

Where

$$< \log(z_k - z_{k0}) > = diag[\log(z_1 - z_{10}),\ \log(z_2 - z_{20}),\ \log(z_3 - z_{30}),\ \log(z_4 - z_{40})]$$

Substituting Eq. (18) into Eq. (17), it is found

$$2\pi[i\mathbf{A}\mathbf{p} + \overline{i\mathbf{A}\mathbf{p}}] = \mathbf{b}^p \tag{19}$$

$$2\pi[i\mathbf{B}\mathbf{p} + \overline{i\mathbf{B}\mathbf{p}}] = \mathbf{f}^p \tag{20}$$

with the aid of Eq. (13), the following relation can be obtained

$$\mathbf{p} = \frac{1}{2\pi i}(\mathbf{A}^t\mathbf{f}^p + \mathbf{B}^t\mathbf{b}^p) \tag{21}$$

4. Force, charge and dislocation interacting with a semi-infinite crack

Consider a semi-infinite mechanically free and electrically open interfacial crack between two bonded dissimilar piezoelectric anisotropic materials. A generalized line dislocation and the generalized line force are applied at a point z_0 in lower half-space. Assume the perfect bonding interface along the positive direction of the x_1-axis and the semi-infinite crack along the negative direction of the x_1-axis (see Fig. 1). The boundary conditions for the current problem are assumed to be written as

$$\begin{cases} \mathbf{u}_a = \mathbf{u}_b \\ \boldsymbol{\phi}_a = \boldsymbol{\phi}_b \end{cases} \quad along\ L_B \qquad (22)$$

$$\begin{cases} \boldsymbol{\phi}_a(z_k) = \mathbf{0} \\ \boldsymbol{\phi}_a(z_k) = \mathbf{0} \end{cases} \quad along\ \ L_C \qquad (23)$$
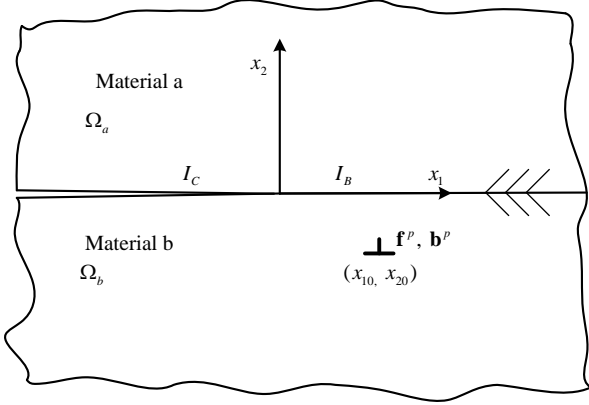

Fig. 1 A singularity in a bimaterial containing a semi-infinite interfacial crack

In some specific boundary conditions, the corresponding points z_k (k=1,2,3,4) of the boundary can be translated into an identical points, e.g. on the x_1-axis or an unit circle, and as a result the boundary equation can be reduced to that containing one variable. In this problem all boundary are along the x_1-axis, the boundary conditions Eqs. (22) and (23) can be rewritten as

$$\begin{aligned} \mathbf{A}_a\mathbf{f}(z) + \overline{\mathbf{A}_a\mathbf{f}(z)} &= \mathbf{A}_b\mathbf{f}(z) + \overline{\mathbf{A}_b\mathbf{f}(z)} \\ \mathbf{B}_a\mathbf{f}(z) + \overline{\mathbf{B}_a\mathbf{f}(z)} &= \mathbf{B}_b\mathbf{f}(z) + \overline{\mathbf{B}_b\mathbf{f}(z)}\ , \qquad z \in I_B \end{aligned} \qquad (24)$$

$$\begin{aligned} \mathbf{B}_a\mathbf{f}(z) + \overline{\mathbf{B}_a\mathbf{f}(z)} &= \mathbf{0} \\ \mathbf{B}_b\mathbf{f}(z) + \overline{\mathbf{B}_b\mathbf{f}(z)} &= \mathbf{0}\ , \qquad z \in I_C \end{aligned} \qquad (25)$$

Introduce a mapping function:

$$\zeta = z^{1/2} \qquad (26)$$

which maps the boundary of crack in z-plane into the imaginary axis in the ζ-plane (Fig. 2). Fortunately, The points of two material along the bonded interface in z-plane still identical in the ζ-plane. The boundary conditions in ζ-plane are written as

$$\begin{aligned} \mathbf{A}_a\mathbf{f}(\zeta) + \overline{\mathbf{A}_a\mathbf{f}(\zeta)} &= \mathbf{A}_b\mathbf{f}(\zeta) + \overline{\mathbf{A}_b\mathbf{f}(\zeta)} \\ \mathbf{B}_a\mathbf{f}(\zeta) + \overline{\mathbf{B}_a\mathbf{f}(\zeta)} &= \mathbf{B}_b\mathbf{f}(\zeta) + \overline{\mathbf{B}_b\mathbf{f}(\zeta)}\ , \qquad along\ \xi_1\ axis\ (\zeta - \overline{\zeta} = 0) \end{aligned} \qquad (27)$$

$$\begin{aligned} \mathbf{B}_a\mathbf{f}(\zeta) + \overline{\mathbf{B}_a\mathbf{f}(\zeta)} &= \mathbf{0} \\ \mathbf{B}_b\mathbf{f}(\zeta) + \overline{\mathbf{B}_b\mathbf{f}(\zeta)} &= \mathbf{0}\ , \qquad along\ \xi_2\ axis\ (\zeta + \overline{\zeta} = 0) \end{aligned} \qquad (28)$$
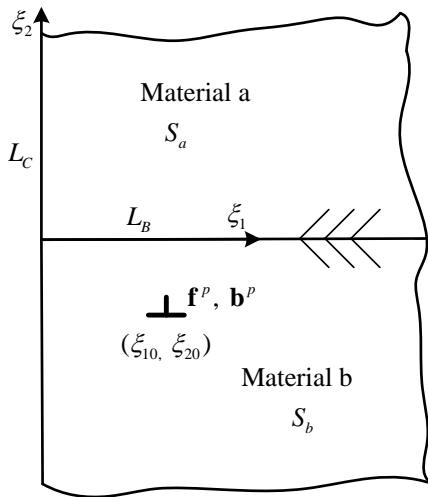

Fig. 2 A singularity in a bimaterial containing a semi-infinite interfacial crack in the mapped plane

Since it is difficult to satisfy both boundary conditions at the same time, the method of analytical continuation should be applied to two boundaries alternatively. First, two perturbed holomorphic functions $\mathbf{f}_{af}(\zeta_k)$ and $\mathbf{f}_{bf}(\zeta_k)$ are introduced to satisfy the continuous conditions of interface L_B. The complex potentials for current problem can be expressed as

$$\mathbf{f}(\zeta_k) = \begin{cases} \mathbf{f}_{af}(\zeta_k) & \zeta \in S_a \\ \mathbf{f}_{bf}(\zeta_k) + \mathbf{f}_0(\zeta_k) & \zeta \in S_b \end{cases} \qquad (29)$$

where S_a, the upper half-space, and S_b, the lower half-space, are occupied by material a and b, respectively, $\mathbf{f}_0(\zeta_k)$ represents the solution of a singularity in a homogeneous medium, in which the piezoelectric material constants of material b are implied in $\mathbf{f}_0(\zeta_k)$. The continuity of mechanical displacement and electric potential across the interface with Eq. (27-1), by analytical continuation arguments, is used to yield

$$\begin{cases} \mathbf{A}_a\mathbf{f}_{af}(\zeta) - \overline{\mathbf{A}_b}\overline{\mathbf{f}_{bf}}(\zeta) - \mathbf{A}_b\mathbf{f}_0(\zeta) = 0 & \zeta \in S_a \\ \overline{\mathbf{A}_a}\overline{\mathbf{f}_{af}}(\zeta) - \mathbf{A}_b\mathbf{f}_{bf}(\zeta) - \overline{\mathbf{A}_b}\mathbf{f}_0(\zeta) = 0 & \zeta \in S_b \end{cases} \qquad (30)$$

The continuity of traction and electric displacement with Eq.

(27-2), by the same arguments, results in

$$\begin{cases} \mathbf{B}_a\mathbf{f}_{af}(\zeta) - \overline{\mathbf{B}}_b\overline{\mathbf{f}_{bf}}(\zeta) - \mathbf{B}_{bf}\mathbf{f}_0(\zeta) = 0 & \zeta \in S_a \\ \overline{\mathbf{B}}_a\overline{\mathbf{f}_{af}}(\zeta) - \mathbf{B}_b\mathbf{f}_{bf}(\zeta) - \overline{\mathbf{B}}_{bf}\overline{\mathbf{f}_0}(\zeta) = 0 & \zeta \in S_b \end{cases} \quad (31)$$

From Eqs. (30) and (31), we have

$$\begin{cases} \mathbf{f}_{af}(\zeta) = \boldsymbol{\alpha}_{ab}\mathbf{f}_0(\zeta) \\ \mathbf{f}_{bf}(\zeta) = \boldsymbol{\beta}_{ab}\overline{\mathbf{f}_0}(\zeta) \end{cases} \quad (32)$$

where

$$\boldsymbol{\alpha}_{ab} = (\overline{\mathbf{A}}_b^{-1}\mathbf{A}_a - \overline{\mathbf{B}}_b^{-1}\mathbf{B}_a)^{-1}(\overline{\mathbf{A}}_b^{-1}\mathbf{A}_b - \overline{\mathbf{B}}_b^{-1}\mathbf{B}_b) \quad (32)$$

The analytical continuation arguments and the property, $\zeta = -\overline{\zeta}$, held along the imaginary axis are used to yield

$$\mathbf{f}_{ah}(\zeta) = -\mathbf{B}_a^{-1}\overline{\mathbf{B}}_a\overline{\boldsymbol{\alpha}}_{ab}\overline{\mathbf{f}_0}(-\zeta_k)$$
$$\mathbf{f}_{bh}(\zeta) = -\mathbf{B}_b^{-1}\overline{\mathbf{B}}_b\overline{\mathbf{f}_0}(-\zeta_k) - \mathbf{B}_b^{-1}\overline{\mathbf{B}}_b\overline{\boldsymbol{\beta}}_{ab}\mathbf{f}_0(-\zeta_k) \quad (36)$$

Similarity, the fields produced by $\mathbf{f}_{ah}(\zeta_k)$ and $\mathbf{f}_{bh}(\zeta_k)$ can not satisfy the continuity conditions at L_B. Two perturbed functions $\mathbf{f}_{af1}(\zeta_k)$ and $\mathbf{f}_{bf1}(\zeta_k)$ are added to satisfy the continuity conditions at L_B. The analytical continuation arguments and the property, $\zeta = \overline{\zeta}$, held along the real axis are used to yield

$$\boldsymbol{\beta}_{ab} = (\overline{\mathbf{B}}_a^{-1}\mathbf{B}_b - \overline{\mathbf{A}}_a^{-1}\mathbf{A}_b)^{-1}(\overline{\mathbf{A}}_a^{-1}\overline{\mathbf{A}}_b - \overline{\mathbf{B}}_a^{-1}\overline{\mathbf{B}}_b) \quad (33)$$

Secondly, two perturbed functions $\mathbf{f}_{ah}(\zeta_k)$ and $\mathbf{f}_{bh}(\zeta_k)$ which are holomorphic in regions S_a and S_b are added to satisfy the mechanically free and electrically open surface L_C. The complex potentials can be expressed as

$$\mathbf{f}(\zeta_k) = \begin{cases} \mathbf{f}_{af}(\zeta_k) + \mathbf{f}_{ah}(\zeta_k) & \zeta \in S_a \\ \mathbf{f}_{bf}(\zeta_k) + \mathbf{f}_0(\zeta_k) + \mathbf{f}_{bh}(\zeta_k) & \zeta \in S_b \end{cases} \quad (34)$$

The boundary condition of mechanically free and electrically open crack surface, Eq. (28), is expressed as

$$\begin{cases} \mathbf{B}_a\mathbf{f}_{af}(\zeta) + \overline{\mathbf{B}}_a\overline{\mathbf{f}_{af}}(\zeta) + \mathbf{B}_a\mathbf{f}_{ah}(\zeta) + \overline{\mathbf{B}}_a\overline{\mathbf{f}_{ah}}(\zeta) = 0 & \zeta \in L_C \\ \mathbf{B}_b\mathbf{f}_0(\zeta) + \overline{\mathbf{B}}_b\overline{\mathbf{f}_0}(\zeta) + \mathbf{B}_b\mathbf{f}_{bf}(\zeta) + \overline{\mathbf{B}}_b\overline{\mathbf{f}_{bf}}(\zeta) + \mathbf{B}_b\mathbf{f}_{bh}(\zeta) + \overline{\mathbf{B}}_b\overline{\mathbf{f}_{bh}}(\zeta) = 0 & \zeta \in L_C \end{cases} \quad (35)$$

$$\begin{cases} \mathbf{f}_{af1}(\zeta) = \boldsymbol{\gamma}_a\overline{\mathbf{f}_0}(-\zeta) \\ \mathbf{f}_{bf1}(\zeta) = \boldsymbol{\gamma}_b\mathbf{f}_0(-\zeta) \end{cases} \quad (37)$$

where

$$\boldsymbol{\gamma}_a = -\boldsymbol{\alpha}_{ab}\mathbf{B}_b^{-1}\overline{\mathbf{B}}_b + \mathbf{B}_a^{-1}\overline{\mathbf{B}}_a\overline{\boldsymbol{\alpha}}_{ab} \quad (38)$$

$$\boldsymbol{\gamma}_b = -\boldsymbol{\beta}_{ab}\overline{\mathbf{B}}_b^{-1}\mathbf{B}_b + \mathbf{B}_b^{-1}\overline{\mathbf{B}}_b\overline{\boldsymbol{\beta}}_{ab} \quad (39)$$

By repeating the previous steps, one can get the other perturbed terms to satisfy both boundary conditions. In the following numerical calculation, we prove that the complex potentials derived as Eq. (40) are well satisfied with the boundary conditions.

$$\mathbf{f}(z_k) = \begin{cases} \boldsymbol{\alpha}_{ab} <\log(\sqrt{z_k} - \sqrt{z_{k0}})> \mathbf{p} - \mathbf{B}_a^{-1}\overline{\mathbf{B}}_a\overline{\boldsymbol{\alpha}}_{ab} <\log(-\sqrt{z_k} - \sqrt{z_{k0}})) > \overline{\mathbf{p}} + \boldsymbol{\gamma}_a <\log(-\sqrt{z_k} - \sqrt{z_{k0}})) > \mathbf{p} \\ \hspace{10cm} \zeta \in S_a \\ <\log(\sqrt{z_k} - \sqrt{z_{k0}}) > \mathbf{p} + \boldsymbol{\beta}_{ab} <\log(\sqrt{z_k} - \sqrt{z_{k0}}) > \overline{\mathbf{p}} - \mathbf{B}_b^{-1}\overline{\mathbf{B}}_b <\log(-\sqrt{z_k} - \sqrt{z_{k0}})) > \overline{\mathbf{p}} \\ -\mathbf{B}_b^{-1}\overline{\mathbf{B}}_b\overline{\boldsymbol{\beta}}_{ab} <\log(-\sqrt{z_k} - \sqrt{z_{k0}}) > \mathbf{p} + \boldsymbol{\gamma}_b <\log(-\sqrt{z_k} - \sqrt{z_{k0}})) > \mathbf{p} \hspace{2cm} \zeta \in S_b \end{cases} \quad (40)$$

For the special case that material a and material b are the same, ($\boldsymbol{\alpha}_{ab} = \mathbf{I}$, $\boldsymbol{\beta}_{ab} = \mathbf{0}$), Eq. (40) reduces to an exact solution of the corresponding problem of a line dislocation interacting with a semi-infinite crack.

4.1. Generalized stress fields

The generalized stress fields can be obtained from Eqs. (14) and (15) as

$$\mathbf{f}(z_k) = <\log(\sqrt{z_k} - \sqrt{z_{k0}}) > \mathbf{p} - \mathbf{B}^{-1}\overline{\mathbf{B}} <\log(-\sqrt{z_k} - \sqrt{z_{k0}})) > \overline{\mathbf{p}} \quad (41)$$

which is in agreement with the result of Chen et al. (2004).

$$\boldsymbol{\sigma}_{1a} = \frac{-1}{\sqrt{z_k}}\mathrm{Re}[\mathbf{B}_a\boldsymbol{\alpha}_{ab} < \frac{p_k}{\sqrt{z_k}-\sqrt{z_{k0}}} > \mathbf{p} - \overline{\mathbf{B}}_a\overline{\boldsymbol{\alpha}_{ab}} < \frac{p_k}{\sqrt{z_k}+\sqrt{z_{k0}}} > \overline{\mathbf{p}} + \mathbf{B}_a\boldsymbol{\gamma}_a < \frac{p_k}{\sqrt{z_k}+\sqrt{z_{k0}}} > \overline{\mathbf{p}}]$$
$$\zeta \in \Omega_a$$

$$\boldsymbol{\sigma}_{1b} = \frac{-1}{\sqrt{z_k}}\mathrm{Re}[\mathbf{B}_b < \frac{p_k}{\sqrt{z_k}-\sqrt{z_{k0}}}) > \mathbf{p} + \mathbf{B}_b\boldsymbol{\beta}_{ab} < \frac{p_k}{\sqrt{z_k}-\sqrt{z_{k0}}} > \overline{\mathbf{p}} - \overline{\mathbf{B}}_b < \frac{p_k}{\sqrt{z_k}+\sqrt{z_{k0}}} > \overline{\mathbf{p}}$$

$$-\overline{\mathbf{B}}_b\overline{\boldsymbol{\beta}_{ab}} < \frac{p_k}{\sqrt{z_k}+\sqrt{z_{k0}}}) > \mathbf{p} + \mathbf{B}_b\boldsymbol{\gamma}_b < \frac{p_k}{\sqrt{z_k}+\sqrt{z_{k0}}}) > \mathbf{p}$$
$$\zeta \in \Omega_b$$

(42)

$$\boldsymbol{\sigma}_{2a} = \frac{1}{\sqrt{z_k}}\mathrm{Re}[\mathbf{B}_a\boldsymbol{\alpha}_{ab} < \frac{1}{\sqrt{z_k}-\sqrt{z_{k0}}} > \mathbf{p} - \overline{\mathbf{B}}_a\overline{\boldsymbol{\alpha}_{ab}} < \frac{1}{\sqrt{z_k}+\sqrt{z_{k0}}} > \overline{\mathbf{p}} + \mathbf{B}_a\boldsymbol{\gamma}_a < \frac{1}{\sqrt{z_k}+\sqrt{z_{k0}}} > \overline{\mathbf{p}}]$$
$$\zeta \in \Omega_a$$

$$\boldsymbol{\sigma}_{2b} = \frac{1}{\sqrt{z_k}}\mathrm{Re}[\mathbf{B}_b < \frac{1}{\sqrt{z_k}-\sqrt{z_{k0}}}) > \mathbf{p} + \mathbf{B}_b\boldsymbol{\beta}_{ab} < \frac{1}{\sqrt{z_k}-\sqrt{z_{k0}}} > \overline{\mathbf{p}} - \overline{\mathbf{B}}_b < \frac{1}{\sqrt{z_k}+\sqrt{z_{k0}}} > \overline{\mathbf{p}}$$

$$-\overline{\mathbf{B}}_b\overline{\boldsymbol{\beta}_{ab}} < \frac{1}{\sqrt{z_k}+\sqrt{z_{k0}}}) > \mathbf{p} + \mathbf{B}_b\boldsymbol{\gamma}_b < \frac{1}{\sqrt{z_k}+\sqrt{z_{k0}}}) > \mathbf{p}$$
$$\zeta \in \Omega_b$$

(43)

4.2. Generalized stress intensity factors

Equations (42) and (43) show that the electro-elastic fields near the crack tip exhibit the $\sqrt{z_k}$ singularity. The generalized stress intensity factors is defined as

$$\mathbf{K} = \left[K_{II}, K_I, K_{III}, K_{D_2} \right]^t = \lim_{\substack{x_1 \to 0 \\ x_2 = 0}} \sqrt{2\pi x_1}\left[\sigma_{21}, \sigma_{22}, \sigma_{23}, D_2 \right]^t$$

(44)

, it can be calculated as

$$\mathbf{K} = \sqrt{2\pi}\,\mathrm{Re}[\mathbf{B}_a\boldsymbol{\alpha}_{ab} < \frac{-1}{\sqrt{z_{k0}}} > \mathbf{p} - \overline{\mathbf{B}}_a\overline{\boldsymbol{\alpha}_{ab}} < \frac{1}{\sqrt{z_{k0}}} > \overline{\mathbf{p}} + \mathbf{B}_a\boldsymbol{\gamma}_a < \frac{1}{\sqrt{z_{k0}}} > \overline{\mathbf{p}}]$$

(45)

or

$$\mathbf{K} = \sqrt{2\pi}\,\mathrm{Re}[\mathbf{B}_b < \frac{-1}{\sqrt{z_{k0}}}) > \mathbf{p} + \mathbf{B}_b\boldsymbol{\beta}_{ab} < \frac{-1}{\sqrt{z_{k0}}} > \overline{\mathbf{p}} - \overline{\mathbf{B}}_b < \frac{1}{\sqrt{z_{k0}}} > \overline{\mathbf{p}}$$

$$-\overline{\mathbf{B}}_b\overline{\boldsymbol{\beta}_{ab}} < \frac{1}{\sqrt{z_{k0}}}) > \mathbf{p} + \mathbf{B}_b\boldsymbol{\gamma}_b < \frac{1}{\sqrt{z_{k0}}}) > \mathbf{p}$$

(46)

4.3. Image force on a piezoelectric dislocation

The image force is defined as the negative gradient of the interaction energy with respect to the position change of the dislocation, which is an important physical quantity for understanding the interacting of a dislocation and interfaces. The image force can be calculated by means of the generalized Peach-Koehler formula by Pak (1990) and Ting and Barnett (1993).

$$F_{x1} = b_{x1}\sigma_{21}^T + b_{x2}\sigma_{22}^T + b_{x3}\sigma_{23}^T + b_{\varphi}D_2^T$$
$$F_{x2} = -(b_{x1}\sigma_{11}^T + b_{x2}\sigma_{12}^T + b_{x3}\sigma_{13}^T + b_{\varphi}D_1^T)$$

(47)

where σ_{ij}^T, and D_i^T are the perturbation stresses and electric displacement components at the dislocation.

$$[\sigma_{21}^T, \sigma_{22}^T, \sigma_{23}^T, D_2^T]^t = \frac{-1}{\sqrt{z_k}} \mathrm{Re}[\mathbf{B}_b \boldsymbol{\beta}_{ab} < \frac{p_k}{\sqrt{z_k}-\sqrt{z_{k0}}} > \bar{\mathbf{p}} - \bar{\mathbf{B}}_b < \frac{p_k}{\sqrt{z_k}+\sqrt{z_{k0}}} > \bar{\mathbf{p}}$$
$$- \bar{\mathbf{B}}_b \overline{\boldsymbol{\beta}_{ab}} < \frac{p_k}{\sqrt{z_k}+\sqrt{z_{k0}}}) > \mathbf{p} + \mathbf{B}_b \boldsymbol{\gamma}_b < \frac{p_k}{\sqrt{z_k}+\sqrt{z_{k0}}}) > \mathbf{p}$$

(48)

$$[\sigma_{11}^T, \sigma_{12}^T, \sigma_{13}^T, D_1^T]^t = \frac{-1}{\sqrt{z_k}} \mathrm{Re}[\mathbf{B}_b \boldsymbol{\beta}_{ab} < \frac{p_k}{\sqrt{z_k}-\sqrt{z_{k0}}} > \bar{\mathbf{p}} - \bar{\mathbf{B}}_b < \frac{p_k}{\sqrt{z_k}+\sqrt{z_{k0}}} > \bar{\mathbf{p}}$$
$$- \bar{\mathbf{B}}_b \overline{\boldsymbol{\beta}_{ab}} < \frac{p_k}{\sqrt{z_k}+\sqrt{z_{k0}}}) > \mathbf{p} + \mathbf{B}_b \boldsymbol{\gamma}_b < \frac{p_k}{\sqrt{z_k}+\sqrt{z_{k0}}}) > \mathbf{p}$$

(49)

5. Numerical results and discussion

For transversely isotropic piezoelectric materials can be classified into two types (Suo et al., 1992). The type I roots p_k ($k=1, 2,3,4$) are all purely imaginary. Of the type II, two roots (p_3 and p_4) are purely imaginary and the other two (p_1 and p_2) have non-zero real parts but with equal imaginary parts. In the follows, we choice two type I piezoelectric materials (PZT-6B and Cadmium selenide) and two type II piezoelectric materials (PZT-4 and PZT-5H) for the numerical discussion. The material properties are listed as follows

PZT-6B:

$c_{11} = 168 GNm^{-2}$, $c_{22} = 163 GNm^{-2}$, $c_{66} = 27.1 GNm^{-2}$, $c_{12} = 60 GNm^{-2}$, $c_{13} = 60 GNm^{-2}$, $e_{21} = -0.9 Cm^{-2}$, $e_{22} = 7.1 Cm^{-2}$, $e_{16} = 4.6 Cm^{-2}$

$\varepsilon_{11} = 3.6 \times 10^{-9} CV^{-1}m^{-1}$, $\varepsilon_{22} = 3.4 \times 10^{-9} CV^{-1}m^{-1}$

Cadmium selenide:

$c_{11} = 74.1 GNm^{-2}$, $c_{22} = 83.6 GNm^{-2}$, $c_{66} = 13.2 GNm^{-2}$, $c_{12} = 39.3 GNm^{-2}$, $c_{13} = 45.2 GNm^{-2}$, $e_{21} = -0.16 Cm^{-2}$, $e_{22} = 0.347 Cm^{-2}$, $e_{16} = -0.138 Cm^{-2}$

$\varepsilon_{11} = 82.6 \times 10^{-12} CV^{-1}m^{-1}$, $\varepsilon_{22} = 90.3 \times 10^{-12} CV^{-1}m^{-1}$

PZT-4:

$c_{11} = 139 GNm^{-2}$, $c_{22} = 113 GNm^{-2}$, $c_{66} = 25.6 GNm^{-2}$, $c_{12} = 74.3 GNm^{-2}$, $c_{13} = 77.8 GNm^{-2}$, $e_{21} = -6.98 Cm^{-2}$, $e_{22} = 13.84 Cm^{-2}$, $e_{16} = 13.44 Cm^{-2}$

$\varepsilon_{11} = 6 \times 10^{-9} CV^{-1}m^{-1}$, $\varepsilon_{22} = 5.47 \times 10^{-9} CV^{-1}m^{-1}$

PZT-5H:

$c_{11} = 126 GNm^{-2}$, $c_{22} = 117 GNm^{-2}$, $c_{66} = 35.3 GNm^{-2}$, $c_{12} = 53 GNm^{-2}$, $c_{13} = 55 GNm^{-2}$, $e_{21} = -6.5 Cm^{-2}$, $e_{22} = 23.3 Cm^{-2}$, $e_{16} = 17 Cm^{-2}$

$\varepsilon_{11} = 15.1 \times 10^{-9} CV^{-1}m^{-1}$, $\varepsilon_{22} = 13 \times 10^{-9} CV^{-1}m^{-1}$.
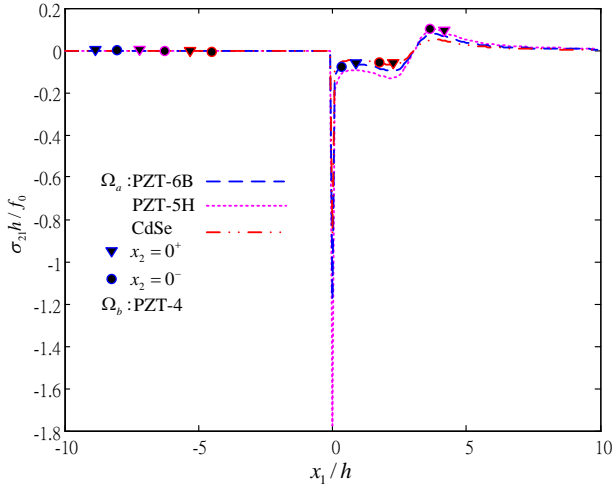
Fig. 3 The distribution of shear stress σ_{21} along x_1-axis

Fig. 4 The distribution of normal stress σ_{22} along x_1-axis

Fig. 5 The distribution of normal stress σ_{23} along x_1-axis
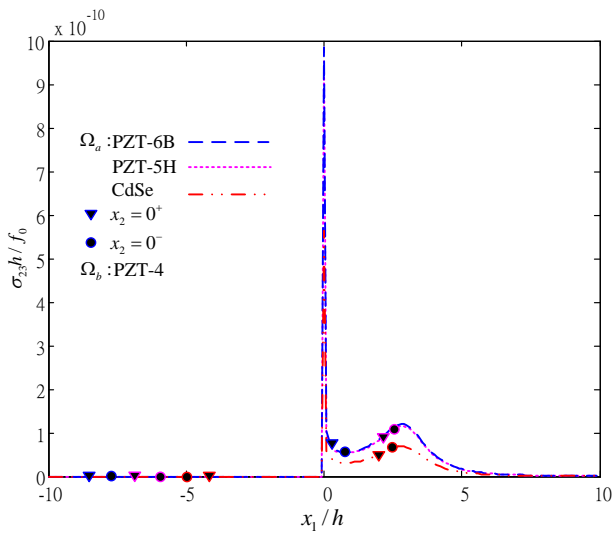
Fig. 6 The distribution of electric displacement D_2 along x_1-axis

Consider a piezoelectric bi-material containing a semi-infinite interfacial crack and is subjected to a line force $\mathbf{f}^p = [0, -f_0, 0, 0]^t$ at the point $z_0 = (3-i)h$. The lower half-plane, Ω_b, is assumed to be PZT-4 and the upper half-plane, Ω_a, may be PZT-5H, PZT-6B or Cadmium selenid. Figures 3-6 show the distributions of generalized interfacial stresses of material a and b along the boundary $x_2 = 0$. From these figures we can find that the shear stress $\sigma_{2,1}$, σ_{23}, normal stress σ_{22} and normal electric displacement D_2 are continuous across the interface and they all vanish along the crack surface. These results prove that the derived solutions are well satisfied with the boundary conditions. Furthermore, one can find the generalized interfacial stresses increase dramatically at the crack tip and increase gradually near the applied load.
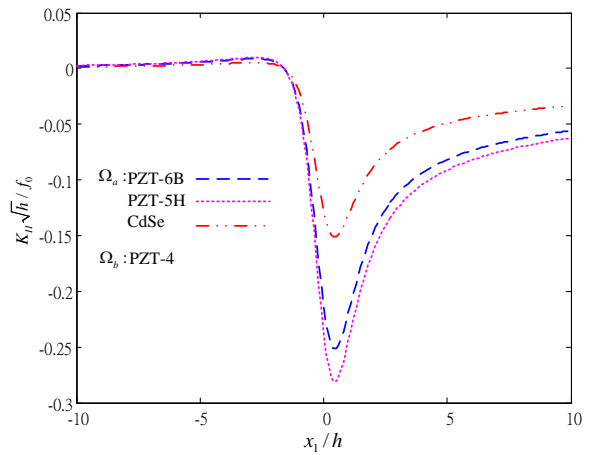
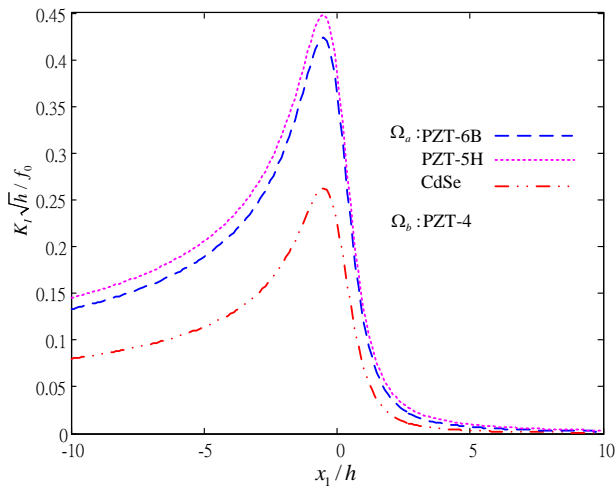**Fig. 7** The distribution of stress intensity factor K_{II}

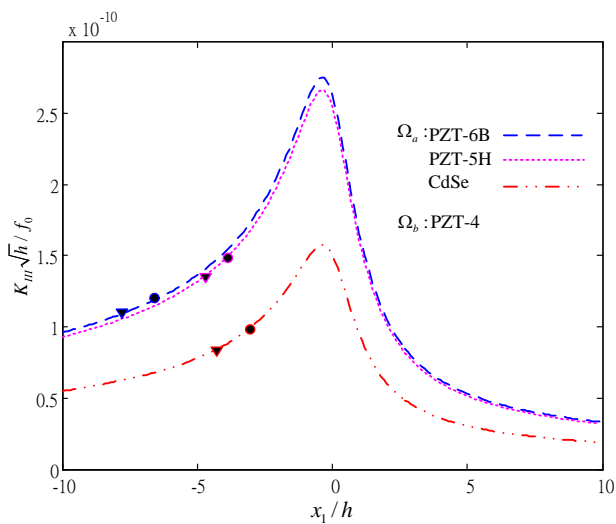**Fig. 8** The distribution of stress intensity factor K_I

Fig. 9 The distribution of stress intensity factor　K_{III}　K_D
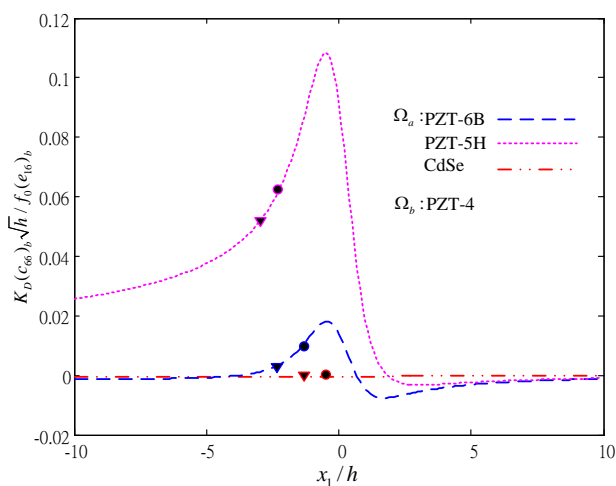

Fig. 10 The distribution of electric displacement intensity

factor

The distributions of generalized stress intensity factors due to the line force applied at the point $z_0 = x_1 - ih$ are plotted in Figs. 7-10, respectively. One can find that the applied load may produce positive or negative generalized stress intensity factors. When the generalized stress intensity factors produced by the line force are positive, it exhibits anti-shielding effect since the generalized stress intensity factors are added to those produced by the far-field loading. On the other hand, when the stress intensity factors produced by the line force are negative, it exhibits shielding effect since the generalized stress intensity factors are subtracted from those produced by the far-field loading. The magnitudes of the generalized stress intensity factors reach a peak value when the line force is applied near the crack tip.　Figs. 11-12 show the distribution of image forces on a dislocation with the Burger vector $\mathbf{b}^p = [0, b_0, 0, 0]^t$ located at the point $z_0 = x_1 - ih$. The negative image force F_{x1} represents the force will attract the dislocation to the cracked side. The positive image force F_{x2} represents the force will attract the dislocation to the interface and the negative image force F_{x2} represents the force will repel the dislocation to the interface. In general, the interface will attract the dislocation when the dislocation locates in one region which is combined with a softer material or a free surface. Oppositely, the interface repels the dislocation when the region is bonded with a harder or rigid material.
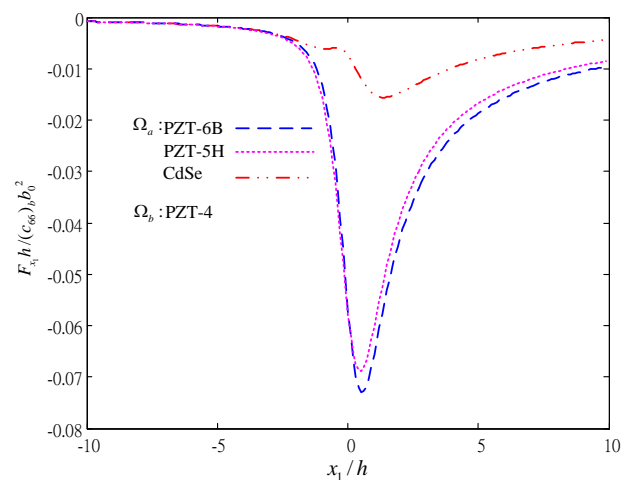

Fig. 11 Dimensionless image forces　F_{x_1}　vs. the position of a
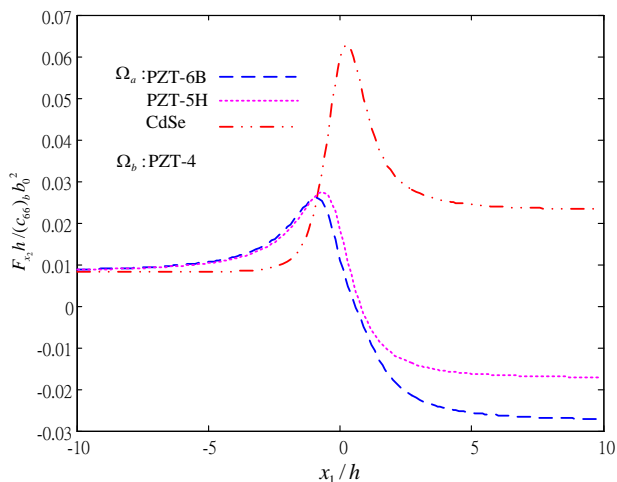
dislocation

Fig. 12 Dimensionless image force F_{x_2} vs. the position of a dislocation

6. Conclusions

The alternating technique and the method of analytical continuation are employed to study the singularities in an anisotropic piezoelectric bonded bi-material containing a semi-infinite interfacial crack. The numerical results prove that the derived solutions are satisfied with the continuity condition at the bonded interface and the mechanically free and electrically open conditions at the crack surface. Then the anti-shielding and shielding effects for loadings and material combinations are discussed. The image forces exerted on a dislocation due to interfaces are estimated by means of the Peach-Koehler formula, which play an important role in the motion of dislocation. Numerical results show that the interfaces will attract the dislocation when the dislocation locates in one region which is combined with a softer material or a free surface. Oppositely, the interface repels the dislocation when the region is bonded with a harder or rigid material.

References

Barnett, D. M., & Lothe, J. (1975). Dislocations and line charges in anisotropic piezoelectric insulators. *Physica Status Solidi B*, 67, 105-111.

Chen, B. J., Xiao, Z. M., & Liew, K. M. (2002). Electro-elastic stress analysis for a wedge-shaped crack interacting with a screw dislocation in piezoelectric solid. *International Journal of Engineering Science*, 40, 621-635.

Chen, B. J., Xiao, Z. M., & Liew, K. M. (2004). A line dislocation interacting with a semi-infinite crack in piezoelectric solid. *International Journal of Solids and Structures*, 42, 1-11.

Chung, M. Y., & Ting, T. C. T. (1996). Piezoelectric solid with an elliptic inclusion or hole. *International Journal of Solids and Structures*, 33, 3343-3361.

Deng, W., & Meguid, S. A. (1999). Closed form solutions for partially debonded circular inclusion in piezoelectric materials, *Acta Mechanica*, 137, 167-181.

Hao, R. J., & Liu, J. X. (2006). Interaction of a screw dislocation with a semi-infinite interfacial crack in a magneto-electro-elastic bi-material. *Mechanics Research Communications*, 33, 415-424.

Hung, Z., & Kuang, Z. B. (2001). Dislocation inside a piezoelectric media with an elliptic inhomogeneity. *International Journal of Solids and Structures*, 38, 8459-8479.

Gao, C. F., Häusler, C., & Balke, H. (2004). Periodic permeable interface cracks in piezoelectric materials. *International Journal of Solids and Structures*, 41, 323-335.

Lee, K. Y., Lee, W. G., & Pak, Y. E. (2000). Interaction between a semi-infinite crack and a screw dislocation in a piezoelectric material. *Journal of Applied Mechanics*, 67, 165-170.

Liu, J. X., Wang, B., & Du, S. Y. (1997). A line force, a line charge and a line dislocation in anisotropic piezoelectric materials with an elliptic hole or crack. *Mechanics Research Communications*, 24, 399-405.

Meguid, S. A., & Deng, W. (1998). Electro-elastic interaction between a screw dislocation and an elliptic inhomogeneity in piezoelectric materials. *International Journal of Solids and Structures*, 35, 1467-1482.

Pak, Y. E. (1990). Force on a piezoelectric screw dislocation. *Journal of Applied Mechanics*, 57, 647-653.

Pak, Y. E. (1992). Linear electro-elastic fracture mechanics of piezoelectric materials. *International Journal of Fracture*, 54, 79-100.

Suo, Z., Kuo, C. M., Barnett, D. M., & Willis, J. R. (1992). Fracture mechanics for piezoelectric ceramics. *Journal of the Mechanics and Physics of Solids*, 40, 739-765.

Ting, T. C. T., & Barnett, D. M. (1993). Image force on line dislocations in anisotropic elastic half-space with a fixed boundary. *International Journal of Solids and Structures*, 30, 313-323.

Wang, X., & Shen, Y. P. (2002). Exact solution for mixed

boundary value problems at anisotropic piezoelectric bimaterial interface and unification of various interface defects. *International Journal of Solids and Structures*, 39, 1591–1619.

Yang, P. S., Liou, J. Y., & Sung, J. C. (2007). Analysis of a crack in a half-plane piezoelectric solid with traction-induction free boundary. *International Journal of Solids and Structures*, 44, 8556-8578.

Yang, P. S., Liou, J. Y., & Sung, J. C. (2008). Infinite sequence of parallel cracks in an anisotropic piezoelectric solid.

Computer Methods in Applied Mechanics and Engineering, 197, 3850-3861.

Zhong, S. M., & Meguid, S. A. (1997). Interfacial debonding of a circular inhomogeneity in piezoelectric materials. *International Journal of Solids and Structures*, 34, 1965-1984.

Zhou, Z. D., Zhao, S. X., & Kuang, Z. B. (2005). Stress and electric displacement analyses in piezoelectric media with an elliptic hole and a small crack. *International Journal of Solids and Structures*, 42, 2803-2822.

奇異點負荷與含半無窮界面裂紋壓電雙材料之交互作用解析研究

沈明河 [1]、洪仕育 [1]、陳世濃 [1]

[1] 南開科技大學　自動化工程系

摘　　要

　　本論文應用延伸之史磋理論探討奇異點負荷與含半無限界面裂紋壓電雙材料之壓電應力交互作用分析。論文所探討的奇異點負荷包括用具平面布格向量之刃狀差排，差排之核心還具有不連續的電勢，集中力，集中電荷等。裂紋表面假設為無曳引力和電氣絕緣狀態。藉由保角轉換函數，解析連續法與交互疊代法，可推導出壓電雙材料各層之壓電應力函數之級數表示式。廣義應力場，廣義應力強度因子和施加在差排之映射力等可以數學方程式明確表示出來，亦可以數值計算繪圖討論。數值計算結果證明在界面結合處及裂紋表面上的邊界條件已完全符合。數值結果亦用來探討奇異點負荷與不同材料組成對於含半無窮界面裂紋之壓電雙材料之廣義之應力函數及廣義之應力強度因子之影響。

關鍵詞：差排、映射力、史磋公式、交替疊代法